# Study of spontaneous aggregation of proteins in the thin gap of a surface force apparatus

**B. Gauthier-Manuel* and J.-P. Gallinet**

*Laboratoire de Physique et Métrologie des Oscillateurs du CNRS associé à l'Université de Franche-Comté, 25044 Besancon Cedex, France*

***Received 13th July 2000, Accepted 15th January 2001***
***First published as an Advance Article on the web 14th February 2001***



We describe a new application of the automatic surface force apparatus to study the spontaneous packing of proteins in a thin gap. With suitable conditions of ionic strength and under a sufficient value of local pressure, spontaneous aggregation of ordered layers of macromolecules occurs. With our experimental setup we observe only a few compact and ordered layers. The development of this technique may lead to another method of crystallizing proteins.

## 1 Introduction

The interactions between a solid surface and proteins are of intense interest in a variety of domains such as biocompatibility of materials,[1] analytical chemistry and many industrial problems.[2]

Proteins are dynamic heterogeneous molecules[3] that have a number of different functions. Some peptides that build the protein have hydrophobic properties while others have hydrophilic ones. Some can be ionized in aqueous solution and present charges of different nature according to the chemical surroundings of the macromolecule.[4–6] The surface charge distribution of proteins is also very heterogeneous and its high-speed variation causes the proteins to adsorb on any surface.[7]

Simultaneous measurements of the interaction force and of the refractive index of the medium lying between two ultrasmooth mica surfaces of a surface force apparatus (SFA) can be a convenient way to study the structure of adsorbed biological macromolecules at the subnanometre level.[8] With this experimental device, we have observed previously[9] a surprisingly well ordered accumulation of the Jackbean lectin, Concanavalin A, that occurs as a function of the local ionic strength in the gap of our automatic SFA. Unfortunately, the ion-diffusion time needed to go from the buffer bulk to the light zone in the middle of the gap of the SFA was about 48 h. The close-packing of the molecules could result from the surface permanent charges of the Concanavalin A dimer[10] and we have explained our experimental results by nucleation of Concanavalin A in the periphery of the gap.[9]

The first steps of the nucleation at the molecular level remain mainly known from theoretical simulations without direct experimental support.[11–13] The real-time following of such a phenomenon with bovine serum albumin shows the universality of compact aggregation in a nanometre-size gap when the ionic strength is slowly increasing so that the variation of the ionic strength in the SFA gap is restricted. We discuss in this paper a likely sequence of aggregation events as a function of the mean refractive index variations in the SFA gap.

## 2 Materials and methods

### 2.1 Materials

The tested protein, bovine serum albumin (BSA), is a small globular protein (66 700 molecular weight) which has never been crystallized.[14] The most common molecular form is a prolate ellipsoid (4.1 nm × 14.1 nm) consisting of about 70% α-helices without β-sheets.[14,15] The molecule shows optical anisotropy.[16,17]

### 2.2 Methods

Interferometry methods have often been used to make advances in the understanding of aggregation steps.[18,19] For that purpose, we have used an automatic SFA as an accurate interferometer with a vertical resolution of about 0.1 nm.[20–22] The timing of the earlier steps of aggregation is inferred from preliminary experiments.[9]

Several modifications of the original measuring device[20] allowed easier use of the SFA. The positions of the silvered mica surfaces are controlled by a servo-looped piezoelectric ceramic in the range 0.1–5000 nm. The automatic data acquisition yields the true distance measured by the FECO ("fringes of equal chromatic order") method with a very high theoretical accuracy (0.1 nm). As the experimenter does not stand near the device during the measurement, thermal drifts are minimized and the experimental accuracy is less than 1 nm. A CCD camera (array of 4096 pixels, 7 μm wide) simultaneously records two consecutive odd and even FECO and thus a mean refractive index $n$ of the medium between the ultrasmooth mica surfaces can be computed. The accuracy on $n$ is 1%.[8,9] The accuracy of the data depends on the quality of the optical signal.

One important parameter is the alignment of the optical elements (Fig. 1) until sharp FECO are formed in the output plane of the spectrometer.[22] As the cleaved mica sheets are birefringent they should be mounted in such a way that the neutral lines are aligned. This can be easily monitored by the use of a polarizing microscope. Good linear dependence of the true distance $D$ between the mica surfaces during the displacement of the lower mica plate (Fig. 1c) is also required. Under these conditions, the correct pair of the two consecutive odd and even FECO always yields a reference value of 1.33 for the refractive index of a diluted solution at large distance.[8,21]

After determination of the reference position by direct contact of the two mica surfaces in air, the surfaces are moved apart and a drop (50 μl) of an aqueous BSA solution (39.6 μg $ml^{-1}$, fraction V, Sigma) is fed at 965 × $10^2$ Pa and 298 K between the mica plates. The BSA solution is then allowed to

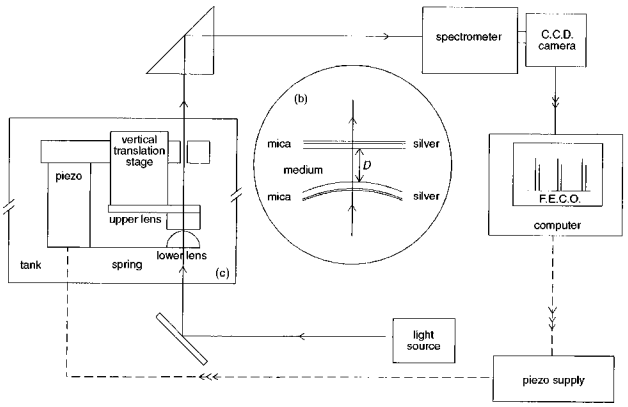


**Fig. 1** Sketch of the automatic surface force apparatus. Upper/lower lens: two freshly cleaved and backsilvered mica plates are glued onto mutually perpendicular cylindrical silica lenses with 2.58 cm radii of curvature. The local geometry of these crossed lenses can be related to a theoretical sphere-plane geometry. Vertical translation stage: motorized actuator for the rough positioning (0.1 μm) of the upper surface. Piezo/spring: piezoelectric servolooped ceramic controls the position of the cantilever spring connected to the lower surface in the range 0.1–5000 nm. Light source: tungsten–halogen lamp. Spectrometer/C.C.D. camera: the optical signal is transmitted through the interferometer, detailed in the inset (b), then dispersed through a prism and a spectrometer and finally produces FECO fringes that are recorded with a CCD camera (array of 4096 pixels, 7 μm wide). Computer: the computer interfaced with the camera continuously records the measurements of the wavelengths of the interference fringes. Piezo supply: computer control of the expansion of the piezoelectric ceramic. (c) Tank: measurement cell filled with water or suitable buffer to eliminate evaporation between the mica surfaces. (b) Details of the confined gap between the crossed cylindrical silica lenses where back-silvered (silver) ultrasmooth mica sheets (mica) are glued. (*D*) True distance between the mica plates. Medium: a drop of a protein solution in water (see Methods) is deposited with a capillary tube between the mica surfaces. The vertical line shows the optical path.

adsorb for 60 min at pH 5.7, a pH value corresponding to the $HCO_3^-/CO_2$ equilibrium in water (alphaQ Millipore). All the solutions are filtered with Whatman Anatop 10 filter (diameter 0.02 μm). The tank of the SFA is then filled with water or with a chosen buffer solution. After thermal equilibrium is obtained the two mica surfaces are slowly brought closer to each other at a velocity as low as 0.1 nm $s^{-1}$ to minimize the hydrodynamic flow and the positions of two consecutive fringes are continuously recorded.

## 3 Experimental results

The results are plotted as $F/R_0$ as a function of the true distance $D$ between the mica surfaces, where $R_0$ is the mean radius of curvature of the surfaces before contact: $R_0 = 2.58$ cm. Thus $F/R_0$ represents the energy of interaction per unit surface between two flat surfaces in the Derjaguin approximation. Unfortunately, the assumption of a constant value for the radius of curvature during the experiment is wrong. Under these conditions the force $F$ as a function of the distance is more pertinent than the energy $F/R_0$. Two ordinate scales $F$ and $F/R_0$ are marked in the force profiles. The computed force profile shows the ejection of the different ordered layers of the adsorbed BSA (Fig. 2). Each of the three jumps is about equal to 4.4 nm according to previous results.[21] Between the levels indicated by the arrows in Fig. 2, corresponding to a jump, intermediary points are computed owing to a defective optical elimination of the lowest component of the birefringent signal.

The mica surfaces are then again separated at a distance of 1 μm. After removing water from the tank, it is refilled with $5 \times 10^{-2}$ M potassium phosphate buffer at pH 7.7. The recording procedure was adapted from a preliminary study of a 3D-ordered protein accumulation induced by slowly changing the ionic strength around the macromolecules.[9] In the narrow confined gap, the actual distance between the silvered mica surfaces and the refractive index of the medium are continuously recorded when the surfaces are drawn closer to each other at a constant fixed velocity (0.12 nm $s^{-1}$). The calculation of the corresponding force is plotted in Fig. 3.

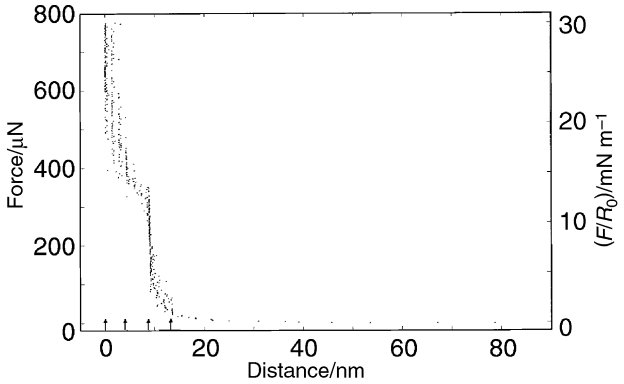


**Fig. 2** Force and energy $F/R_0$ between two mica plates coated with adsorbed BSA molecules as a function of the true distance $D$ (see Fig. 1(b)) between the mica surfaces. A 50 μl droplet of BSA solution (39.6 μg $ml^{-1}$, fraction V, Sigma) is placed between the two mica surfaces. The measurement cell (tank, Fig. 1) is filled with alphaQ Millipore water (pH 5.7, $p = 965 \times 10^2$ Pa, $T = 298$ K). The arrows show the position of the mica surfaces after each jump during the compression stress. Approach velocity of the mica surfaces = 0.06 nm $s^{-1}$; fringe order = 47; 1546 points.

In the first stage the distance between the surfaces decreases and the layers of molecules are ejected. The compression force at pH 7.7 with the phosphate buffer exceeds the preceding value (600 μN) obtained at pH 5.7 (Fig. 2). The movement of the lenses is stopped at a minimal constant distance (8.5 nm, Fig. 3 and time = 0 in Fig. 4) which corresponds to the thickness of two side-on oriented BSA molecules. Thus the two last layers of BSA are not ejected. Fig. 4(a) is a plot of the distance $D$ (*cf.* Fig. 1(b)) *vs.* time and corresponds to the plot of the force profile of Fig. 3. As the molecules are charged, the ejection of layers is seen as a smooth increase of the force. The mean refractive index of the two adsorbed BSA layers is found to be equal to $1.7 \pm 0.1$ (Fig. 4(b)). This corresponds to a dense packing of the molecules.[16,17] Unfortunately, the aggregates of protein are now too small for an accurate experimental determination of the refractive index and only a few computed values are known.[23,24]

At 600 μN, the distance between the two lenses suddenly increases against the compression force. This second stage begins at approximately 10 800 s and the distance between the surfaces increases with successive discontinuities (Fig. 4(a)). At

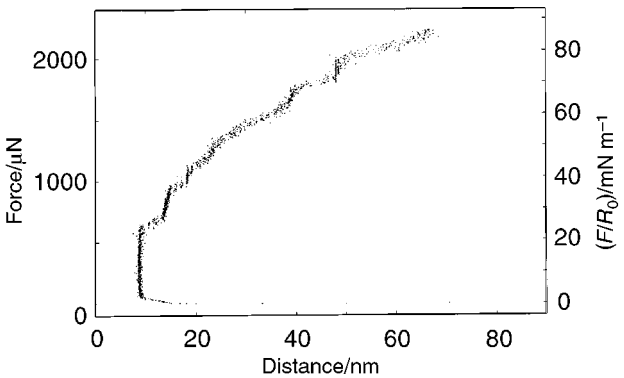


**Fig. 3** The interaction force and energy $F/R_0$ as a function of the true distance between the two back-silvered mica plates coated with BSA as in the preceding figure and in contact with a $5 \times 10^{-2}$ M phosphate buffer, pH 7.7 (see details in text). Imposed approach velocity of the mica plates = 0.12 nm $s^{-1}$; fringe order = 47; 4095 points.

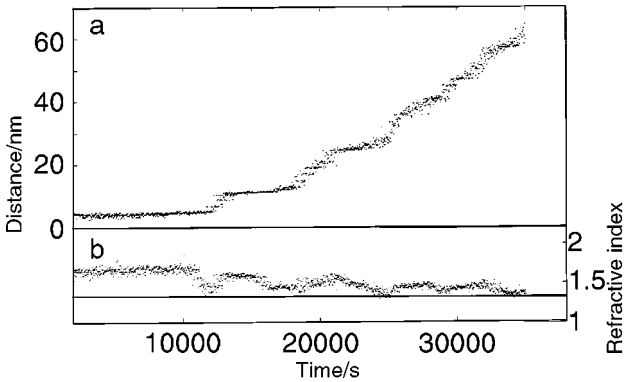


**Fig. 4** Concomitant variations (*vs.* time) of the true distance between the two mica plates and of the refractive index of the protein layers confined between the two mica surfaces. (a) Increasing the true distance between the mica sheets against the compression stress (approach velocity = 0.12 nm $s^{-1}$) imposed by the servolooped device of the piezoelectric ceramic that moves the lower mica plate fixed on a cantilever. This profile corresponds to the force profile of Fig. 2 when the force is $\geqslant$50 μN. (b) Concomitant fluctuations of the refractive index of the medium illuminated by white light in the gap of the SFA (interferometric FECO method). Index computed from the two fringes 46 and 47. Experimental conditions as in Fig. 3.

each discontinuity a new layer of molecules is introduced in the gap against the compression motion. If we carefully examine in Fig. 4(b) the behaviour of the refractive index during the first discontinuity of the distance, we see that in a first step its value decreases to approximately 1.33 and then increases in a second step to a slightly lower value than previously. This means that a new layer of molecules comes from the outside of the gap, separates the surfaces, and migrates to the center.

As time advances the inserted layers are less and less ordered as can be deduced from the decrease in the mean value of the refractive index. We can suppose that the compressive force, induced by the external movement, is too small to order a great number of layers. Some further experiments are necessary to adjust the compressive force to the number of layers in the aggregate and to obtain an object able to be studied by diffraction. Thus we observe here the same behaviour as with Concanavalin A.[9]

At the end of the experiment, when the surfaces are moved apart against the external compressive force, the central zone of the interferometer is flattened, to give a quasi-planar zone of radius 50 μm.[9] This zone, observed with monochromatic light at $\lambda$ = 580.7 nm (Fig. 5), shows optical heterogeneities in the central part of the Newton rings. The central zone is non-uniform as would be expected. A yellow near-central zone confirms the presence of matter with different refractive index

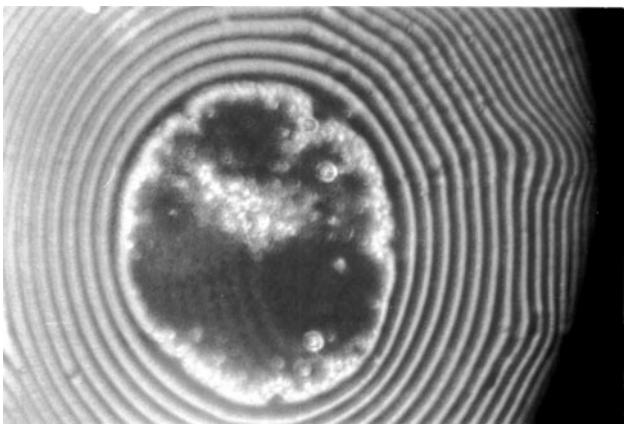

**Fig. 5** Visualization of the central part of the interferometer to detect local variation of the refractive index owing to protein aggregates. Monochromatic light image ($\lambda$ = 580.7 nm).

and confirms the preceding results deduced from force and refractive index measurements (*cf.* Fig. 4). Near the first ring several aggregates are also clearly seen. The clusters deform the monochromatic rings proving a local change in the refractive index.

## 4 Discussion

These observations can be explained by the mechanism proposed in Fig. 6. From the profiles of Fig. 4 at a time less than 10 000 s, the initial state (Fig. 6(a)) corresponds to the two protein monolayers that are closest packed on the mica surfaces. In the first step (Fig. 6(b)), the adsorbed protein layer migrates from the center of the gap to nourish a seed center outside the optically measured area. The refractive index decreases to 1.33, the value of water.

The second step (Fig. 6(c)) is characterized by further growth of the initial aggregation center that pushes the mobile mica surface glued to the silica lens fixed on the cantilever. This expansion of the gap allows the arrival of more BSA molecules from the solution to be adsorbed on the vacant sites of the mica surfaces (Fig. 6(d)). Thus, the refractive index of the medium increases. After the first jump, the gap consists of two layers of adsorbed proteins and a layer of water, all of the same thickness. A rough evaluation of the refractive index is $n^* = (1.7 \times 2/3) + (1.33 \times 1/3) = 1.58$, in agreement with the experimental data of Fig. 4(b) at the time around 15 000 s.

The following successive jumps with regular steps of 4.5 nm lead to less ordered layers because the compression stress increases too slowly to orient the BSA molecules in the same position in the new layers. An approximate value of the force, that is required to order a layer and corresponding to the geometry of that experiment, can be estimated from Fig. 4: 600 μN for two layers and 1000 μN for three layers. Thus a local force around 300 μN is likely required to order a layer.

The interesting quantity is the force per unit surface area but this information is very difficult to obtain because of deformation of the surfaces under the pressure stresses.[25,26] In that configuration, the surfaces are partly deformed[9] and we cannot measure the actual radius of curvature of the surfaces. Such surface deformations greatly change the local radius of curvature of the mica surfaces and the classical parameter $F/R$ computed without deformation becomes inadequate.

However, the local pressure inside the gap is a fundamental parameter. We have observed that when the surfaces are brought together in the presence of charged proteins: partly

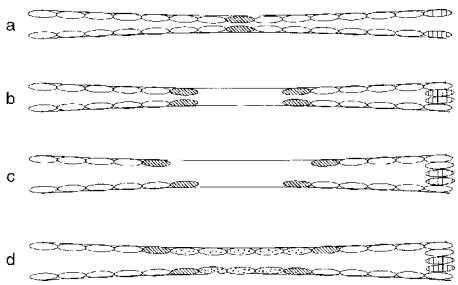


**Fig. 6** Schematic mechanism of the early steps of the aggregation and growth of the BSA clusters. (a) The ordered pattern of adsorbed molecules of the BSA prolate ellipsoids (white ellipsoids) yields maximal attractive forces that becomes higher than the adsorption force, as seen in Fig. 4(b) at 10 000 s. (b) Desorbed BSA molecules (hatched ellipsoids) and BSA molecules moving to the peripheral aggregation centers. The refractive index decreases with no displacement of the mica sheets (see Fig. 4(b) at 10 800 s). (c) Desorbed molecules (vertical hatched ellipsoids) induce growth of the aggregation clusters causes a jump of the mica surfaces against the compression stress imposed by the cantilever of the SFA. (d) BSA molecules of the outer protein solution enter the gap and new molecules (dotted ellipsoids) adsorb onto the free mica surfaces.

disordered multilayers of proteins yield a refractive index of 1.5–1.6. After a constant compression stress for 48 h, these layers adopt a closer packing which is characterized by a great decrease in the distance between the surfaces and the refractive index reaches a high value of 1.7.[9] From the new molecular packing, an ordered accumulation seems to occur if the pH is changing by diffusion of ions to the isoelectric point $pH_i$ of the protein.[9] This phenomenon is again observed here with BSA, a malleable protein that easily aggregates.[27,28]

The process of aggregation is favored by the size of the gap. The Debye length associated with the ionic strength of the surrounding medium, 0.05, is equal to 1.4 nm. To obtain a spatially ordered 3D arrangement of a charged molecule upon the first adsorbed BSA layer, the free space in the gap must be greater than the mean height of 4.4 nm observed at the $pH_i$ of the protein with a double layer of counterions of about 1.4 nm. The observed 6.0 nm first jump against the compression stress fits such an assumption (Fig. 3 and Fig. 4(a) at time 12 500 s). The transitions between the jumps are smooth when the proteins are charged (Fig. 3) while the variations in the distance are sharp at the BSA $pH_i$ (Fig. 2).

The start of aggregation and the subsequent growth of the ordered macromolecular clusters are energetically unfavorable.[29,30] The clusters will generally dissociate. The imposed compression stress ($\leqslant$25 μN) could likely contribute to cancellation of the gravity-induced convection in the ultrathin gap ($\leqslant$9 nm, Fig. 3). When the diffusion of the buffer ions leads to a concentration gradient of counterions around the protein molecules, then these counterions are stabilized at a mean distance.

The $pH_i$ of commercial preparations of BSA is about 4.7–5.0, depending on the method of preparation.[4,31] In an open atmosphere, the dilute aqueous solution of BSA is at pH 5.7, a pH controlled by the dissolved atmospheric $CO_2$. At this experimental stable equilibrium, many proteins have a very low global charge but their surface is a mosaic of moving (+) and (−) charges.[3,32] Due to the counterion layer on the BSA molecules, surface charges are counteracted so that after a while the proteins will not be able to "jiggle", thus favouring a periodic packing onto the preexisting compactly adsorbed layer where the BSA molecules are fixed by contact with the mica surface. Such a favorable zone can be located only at the level of a torus where the height of the gap permits molecule accumulation (Fig. 6).

Thus, another important parameter is the very slow diffusion of ions in the gap from the periphery. It allows ionic surroundings which leads to nucleation. This agrees with observations on concentrated solutions of proteins: random aggregation is avoided with a pH far away from the $pH_i$ (repulsive interactions) and ordered accumulation is induced when the pH is near to the $pH_i$ (attractive interactions).[6,33]

## 5 Summary

An automatic surface force apparatus presents many advantages for simultaneously studying several parameters that control the adsorption of proteins. The interactions between the mica surfaces and the proteins stabilize the molecular geometry and the narrowness of the gap prevents convection phenomena. The slow diffusion of externally added ions allows a sufficient decrease in the motions of the protein molecules to favor an ordered packing in the gap between the two silica lenses of the device. This phenomenon stops the imposed movement of the SFA lenses and restricts the range of the ionic strength variation.

## Acknowledgements

This work was partly supported by the CNRS (GDR 1092: "interactions faibles: solutions concentrées et cristallogénèse des macromolécules biologiques").

## References

1 J. D. Andrade, V. Hlady, L. Feng and K. Tingey, in *Interfacial Phenomena and Bioproducts*, ed. J. L. Brash and P. W. Wojciechowski, Marcel Dekker, New York, 1996, ch. 2, p. 19.
2 J. J. Ramsden, *Quart. Rev. Biophys.*, 1994, **27**, 41.
3 M. Karplus and J. A. McCammon, *Annu. Rev. Biochem.*, 1983, **53**, 263.
4 M. M. Ries-Kautt and A. F. Ducruix, *J. Biol. Chem.*, 1989, **264**, 745.
5 T. Simonson and C. L. Brooks, *J. Am. Chem. Soc.*, 1996, **8bf 118**, 8452.
6 A. Tardieu, A. Leverge, M. Malfois, F. Bonneté, S. Finet, M. Ries-Kautt and L. Belloni, *J. Cryst. Growth*, 1999, **196**, 193.
7 J. J. Ramsden, *Chem. Soc. Rev.*, 1995, 73.
8 B. Gauthier-Manuel and J.-P. Gallinet, *J. Colloid Interface Sci.*, 1995, **175**, 476.
9 B. Gauthier-Manuel and J. P. Gallinet, *Langmuir*, 1997, **13**, 2541.
10 J.-P. Gallinet and B. Gauthier-Manuel, *Eur. Biophys. J.*, 1993, **22**, 195.
11 G. Feher and Z. Kam, *Methods Enzymol.*, 1985, **114**, 77.
12 R. C. DeMattei and R. S. Feilgelson, *J. Cryst. Growth*, 1992, **122**, 21.
13 H. Riveros, E. Cabrera, M. Gally, C. Ruiz-Mejia and J. Fujioka, *J. Cryst. Growth*, 1993, **128**, 44.
14 D. C. Carter, B. Chang, J. X. Ho, K. Keeling and Z. Krishnasami, *Eur. J. Biochem.*, 1994, **226**, 1049.
15 D. C. Carter and J. X. Ho, *Adv. Protein Chem.*, 1994, **45**, 153.
16 M. Andersen and L. R. Painter, *Biopolymers*, 1974, **13**, 1261.
17 Y. Sano, *J. Colloid Interface Sci.*, 1988, **124**, 403.
18 K. Onuma, K. Tsukamoto and S. Nakadate, *J. Cryst. Growth*, 1993, **129**, 706.
19 E. H. Snell, J. R. Helliwell, T. J. Boggon, P. Lautenschlager and L. Potthast, *Acta Crystallogr., Sect. D: Biol. Crystallogr.*, 1996, **52**, 529.
20 J. N. Israelachvili, *Intermolecular and Surface Forces*, Academic Press, London, 2nd edn., 1992.
21 J.-P. Gallinet and B. Gauthier-Manuel, *Colloids Surf.*, 1992, **68**, 189.
22 B. Gauthier-Manuel and J.-P. Gallinet, *Biochimie*, 1998, **80**, 391.
23 S. Dejong, F. Groeneweg and F. V. Vader, *J. Appl. Crystallogr.*, 1991, **24**, 171.
24 A. L. Guerrero, C. Sainz, H. Perrin, R. Castell and J. Calatroni, *Opt. Laser Technol.*, 1992, **24**, 333.
25 A. M. Stewart, *J. Colloid Interface Sci.*, 1995, **170**, 187.
26 H. K. Christenson, *Langmuir*, 1996, **12**, 1404.
27 A. N. Asanov, L. J. De Lucas, P. B. Oldham and W. W. Wilson, *J. Colloid Interface Sci.*, 1997, **191**, 222.
28 A. N. Asanov, L. J. De Lucas, P. B. Oldham and W. W. Wilson, *J. Colloid Interface Sci.*, 1997, **196**, 62.
29 D. M. Blow, N. E. Chayen, L. F. Lloyd and E. Saridakis, *Protein Sci.*, 1994, **3**, 1638.
30 O. Galkin and P. G. Vekilov, *J. Am. Chem. Soc.*, 2000, **122**, 156.
31 P. G. Righetti and T. Caravaggio, *J. Chromatogr.*, 1976, **127**, 1.
32 T. Egawa and T. Masuda, *Biochim. Biophys. Acta*, 1989, **995**, 207.
33 S. Finet, F. Bonneté, J. Frouin, K. Provost and A. Tardieu, *Eur. Biophys. J.*, 1998, **27**, 263.